
^{40}Ar - ^{39}Ar Ages and Irradiation History of Luna 24 Basalts

J. Hennessy and G. Turner

Phil. Trans. R. Soc. Lond. A 1980 **297**, 27-39

doi: 10.1098/rsta.1980.0202

Email alerting service

Receive free email alerts when new articles cite this article - sign up in the box at the top right-hand corner of the article or click [here](#)

To subscribe to *Phil. Trans. R. Soc. Lond. A* go to:
<http://rsta.royalsocietypublishing.org/subscriptions>

^{40}Ar – ^{39}Ar AGES AND IRRADIATION HISTORY OF LUNA 24 BASALTS

BY J. HENNESSY AND G. TURNER*

*Department of Physics, University of Sheffield,
Sheffield S3 7RH, U.K.*

Communicated by G. Eglinton, F.R.S. – Received 21 February 1979 – Revised 26 October 1979)

CONTENTS

	PAGE
INTRODUCTION	28
EXPERIMENTAL METHODS	29
RESULTS AND DISCUSSION	30
Crystallization and cooling ages	30
Cosmic ray exposure history	34
Deposition history of the Luna 24 regolith	37
SUMMARY AND CONCLUSIONS	38
REFERENCES	39

The Luna 24 mission sampled a variety of lithologies in a single core. Two of these lithologies, a metabasalt (24196) and a crushed basalt (24170) have been subjected to ^{40}Ar – ^{39}Ar dating experiments to determine if metamorphism significantly post-dated basalt extrusion.

The metabasalt exhibited symptoms of both solar wind contamination and ^{39}Ar recoil; in view of these effects an age may only be defined by making extreme assumptions. High temperature release fractions give an age of 3.36 ± 0.11 Ga, while the cumulate $^{40}\text{Ar}/^{39}\text{Ar}$ ratio gives 3.14 ± 0.16 Ga; both are comparable with the basalt (24170) age and suggest that the metabasalts represent thermally penecontemporaneously metamorphosed flow margins, rather than the products of later impact events.

The feldspar from the microgabbro yielded an age of 3.37 ± 0.20 Ga. The ratios of cosmogenic ^{38}Ar to Ca in pyroxene and feldspar are within error identical, indicating that ^{38}Ar production from Fe in the pyroxene is small. This is the first definitive use of Fe-produced ^{38}Ar as a spectral hardness indicator and implies that the microgabbro received much of its cosmic ray exposure at depth in the regolith. By taking account of the dependence of ^{38}Ar production rate with depth it is inferred that the microgabbro layer was deposited within the last 350–500 Ma. By implication, the regolith layers above the microgabbro at the Luna 24 site are younger. The metabasalt has an identical cosmogenic $^{38}\text{Ar}/\text{Ca}$ ratio; however, because of the decrease of production rate with depth it could have experienced a 20% pre-exposure before deposition of the microgabbro.

Spectral information has also been obtained from a reappraisal of published argon data and indicates a much harder spectrum for a near surface sample. The way in which the Ca- and Fe-produced $^{38}\text{Ar}_c$ follow the broad trend of the instantaneous production profiles suggests that the regolith at the Luna 24 site has been relatively undisturbed for much of the last 300 Ma.

* Elected F.R.S. 20 March 1980.

INTRODUCTION

The third Soviet unmanned lunar return mission, Luna 24, retrieved material from the south-eastern region of Mare Crisium. The general geology of Mare Crisium is shown in figure 1, which has been adapted from Head *et al.* (1978). Four major units have been defined by orbiter remote sensing and telescope studies; from oldest to youngest these are groups I, IIb, IIa and III. Group I basalts are seen as a relatively mature soil with TiO_2 current around 4% at the basin margin, to the southeast of the Luna 24 landing site. The ejecta from several

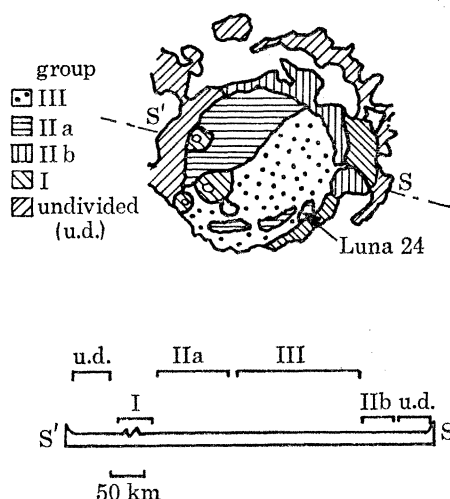


FIGURE 1. Geological units of Mare Crisium (adapted from Head *et al.* 1978).

nearby craters may form a significant component in the soil of this region. Group IIa is a very low-titanium iron-rich basalt, and occurs as infill in the northwestern part of the basin, and in a series of irregular patches to the southeast. Group IIb, differentiated from IIa by its absorption characteristics at $1 \mu\text{m}$, forms the easterly and northeasterly margins of the basin; evidence of onlap by group IIa shows group IIb to be the elder. The final unit, group III, onlaps all the older units, but is thin in places, as evidenced by the exposed group IIa patches. Luna 24 sampled one of the group IIa patches, just to the southeast of the crater Fahrenheit.

Detailed petrological studies by a number of research groups indicate a variety of components in the Luna 24 soil. Taylor *et al.* (1978), for example, list the following lithologies. (1) Ferrobasalts with ophitic to subophitic textures and bulk compositions which are Fe-rich, Mg- and Ti-poor. These have been variously referred to as 'VLT' (very low Ti) mare basalts. (2) Metabasalts with very fine grained ($25 \mu\text{m}$) granulitic textures. These have bulk compositions similar to the ferrobasalts and appear to be thermally metamorphosed ferrobasalts (Ryder *et al.* 1977). (3) Ferrogabbros, which appear to be coarse-grained versions of the ferrobasalts. (4) Mg-rich gabbros, represented mainly among monomineralic fragments in the soil. (5) Olivine-rich fragments, frequently with vitrophyric textures. (6) A relatively minor component of non-mare fragments, many of which are shock melted and were presumably transported to the Luna 24 site by impacts in surrounding (or underlying) terra regions. The bulk chemistry of the soil is remarkable in that it is richer in Mg (*ca.* 10% MgO) (Blanchard *et al.* 1977; Ma & Schmitt 1977) than the most abundant lithic fragments (6–7% MgO). A possible explanation

advanced to account for this is that the extra Mg is present in an older, more degraded VLT basalt which is under-represented in the size fractions of lithic fragments studied petrographically.

The radiometric chronology of the Luna 24 site currently rests on age determinations of only four rock fragments: a microgabbro, 24170, with an age of 3.30 ± 0.05 Ga (^{40}Ar – ^{39}Ar and Sm–Nd; Lunatic Asylum 1978); a fine grained VLT basalt from layer 24096, with an age of 3.60 ± 0.12 Ga (^{40}Ar – ^{39}Ar ; Stettler & Albarede 1978), and two basalt fragments from layer 24077, with ages of 3.24 ± 0.06 Ga and 3.33 ± 0.21 Ga (^{40}Ar – ^{39}Ar ; Schaeffer *et al.* 1978). Only in the microgabbro, 24170, were the argon measurements unaffected by the presence of solar wind argon and of a precision comparable with that of the more numerous Apollo age measurements (made on samples two orders of magnitude larger).

In an attempt to extend this chronology, ^{40}Ar – ^{39}Ar dating experiments have been carried out on samples from two horizons in the Luna 24 core. By analysis of the largest fragment, a metabasalt from level 24196, we hoped to answer the question ‘Did the metamorphism of the metabasalts occur significantly later than the extrusion of the Mare Crisium lavas, as represented by 24170?’ An alternative, but less likely, possibility, that they represent the effects of thermal metamorphism following a local impact, would not require extrusion and metamorphism to be contemporaneous.

In addition to the metabasalt study we have also analysed two mineral separates from the microgabbro, 24170. The major interest in this analysis rests in a comparison of cosmic ray-produced ^{38}Ar in feldspar and pyroxene, which can be used to determine relative production rates of ^{38}Ar from Ca and Fe. Since production from Fe requires considerably more energetic cosmic ray protons than production from Ca, the analysis can be used to provide spectral information which, together with cosmogenic $^{38}\text{Ar}/\text{Ca}$ ratios, is relevant to the deposition history of the Luna 24 core.

EXPERIMENTAL METHODS

The largest of the two samples analysed, 24196,1,9011, a 17 mg fragment, was broken into three pieces. Of these, one, 4 mg in mass, was subjected to a microprobe analysis (Graham & Hutchison 1980, this volume) and the two other pieces (6 and 7 mg) were subjected to ^{40}Ar – ^{39}Ar analysis. 24170,1–3, a crushed microgabbro, has been described in detail by the Lunatic Asylum (1978); it consists of angular pyroxene and feldspar fragments, with a small percentage of olivine. Petrographic and isotopic evidence suggests that the material represents a single rock. Two mineral separates of feldspar (2.5 mg) and pyroxene (3 mg) were prepared for argon analysis by hand picking.

All samples were packaged in aluminium foil and evacuated Vitrosil tubes, and irradiated in the Herald reactor at A.W.R.E., Aldermaston. J values ($J = (e^{\lambda t} - 1)/(^{40}\text{Ar}/^{39}\text{Ar})$) were measured by using aliquots of our standard hornblende monitor, Hb3gr ($t = 1.072 \pm 0.02$ Ga; Turner *et al.* 1971, 1978) packaged with the samples in the Vitrosil tubes. The spatial variation in fluence was also monitored by Ni flux wires spaced around the sample container. The irradiation canister was rotated through 180° half way through the irradiation, but in spite of this J values in the different sample tubes ranged from 0.0954 ± 0.0003 (24170 pyroxene) to 0.1046 ± 0.0010 (24170 feldspar).

Stepped heating experiments were performed by using a miniature extraction system built recently to reduce ^{40}Ar system blanks. The furnace is similar to that described by Staudacher

et al. (1978) and consists essentially of a double vacuum system, the outer vacuum containing the heater element, the sample being in a smaller inner ultra-high-vacuum enclosure constructed of tantalum. Extraction blanks range from 10^{-10} cm³ (at s.t.p.) at low temperatures to 5×10^{-10} cm³ (at s.t.p.) at 1500 °C. The total volume of the extraction system and its associated sample loader is of the order of 50 cm³.

Argon isotopes were measured on a 15 cm 90° sector focusing mass spectrometer by using electrometer detection of the ion beam with a 100 GΩ resistor. Currently there is no provision for electron multiplier ion detection and the precision of age determinations on very small K-poor rocks such as the Luna 24 samples is in consequence limited in roughly equal parts by the ⁴⁰Ar blank and the signal:noise ratio of the small ³⁹Ar peak.

The results discussed in the next section and displayed in the figures have been corrected for spectrometer discrimination, ³⁷Cl background, decay of ³⁷Ar and interfering neutron-induced reactions. Ages quoted have been derived by using the I.U.G.S. recommended decay constants and isotopic abundances for potassium (Steiger & Jäger 1977), $\lambda_{\beta} = 4.962 \times 10^{-10}$ a⁻¹, $\lambda_{\epsilon} = 0.581 \times 10^{-10}$ a⁻¹, ⁴⁰K/K = 0.011 67 at. %.

RESULTS AND DISCUSSION

Argon isotopes in neutron-irradiated lunar rocks provide information about crystallization and cooling times (by way of ⁴⁰Ar/³⁹Ar) and cosmic ray exposure (by way of ³⁸Ar/³⁷Ar). These two aspects are discussed separately below. Corrections are necessary in both cases for the presence of solar wind implanted 'trapped' argon. These are made by the use of isotope correlation diagrams and, where appropriate, by the additional assumptions that (³⁸Ar/³⁶Ar)_e = 1.63 (cosmogenic ratio) and (³⁸Ar/³⁶Ar)_t = 0.1869 (trapped ratio).

Crystallization and cooling ages

The argon isotope ratios relevant to the ⁴⁰Ar–³⁹Ar chronology of the two fragments of 24196,1,9011 are displayed in figure 2, which is a ³⁶Ar_t/⁴⁰Ar–³⁹Ar/⁴⁰Ar isotope correlation diagram. For convenience the fragments will be referred to as 24196A (the 7 mg fragment) and 24196B (the 6 mg fragment, analysed first). In this representation, trapped argon is plotted on the abscissa while potassium-derived argon is plotted on the ordinate (ages decreasing to the right). The experimental points are mixtures of both components.

Aside from the 870 °C point from 24196B, which is discussed below, the data follow a pattern typical of lunar soil fragments. The low-temperature argon is dominated by solar wind implantation with the points lying close to the abscissa. The ⁴⁰Ar/³⁶Ar ratio of this trapped argon decreases as the extraction temperature increases reflecting the fact that the mean implantation depth of re-trapped ⁴⁰Ar is less than that of the true solar wind ³⁶Ar. Such a variation has been observed several times previously (see, for example, Cadogan & Turner 1977) and points to the danger inherent in the common assumption of a 'nominal' (⁴⁰Ar/³⁶Ar)_t ratio when determining ⁴⁰Ar–³⁹Ar ages. The ³⁹Ar released during this initial phase is between 20 and 30 % of the total and cannot be used to obtain age information.

Above 900 °C, the points move to the right as radiogenic argon is released; however, the ages implied by the 950 °C (B), 1020 °C (A) and 1090 °C (A) points are lower than those of the high-temperature release, a feature which would conventionally be interpreted as the effect of diffusive loss of radiogenic ⁴⁰Ar. The four high-temperature points correspond to ages of

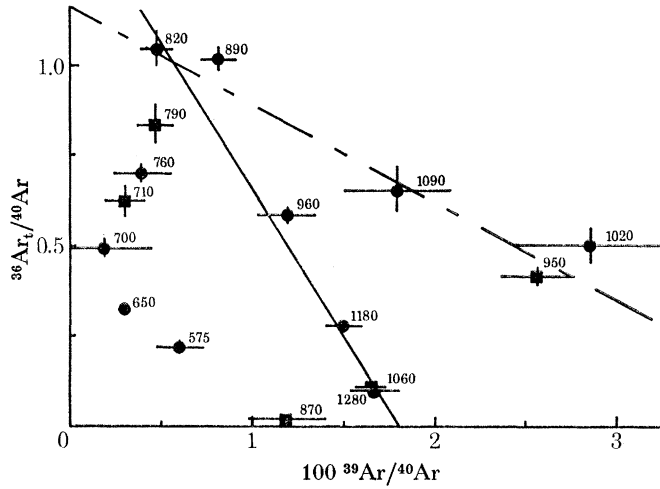


FIGURE 2. $^{36}\text{Ar}_t/^{40}\text{Ar}$ - $^{39}\text{Ar}/^{40}\text{Ar}$ isotope correlation diagram for 24196A (circles) and 24196B (squares). Trapped argon compositions are plotted on the abscissa, potassium derived argon on the ordinate. The experimental points represent binary mixtures of both components with trapped argon dominating at low temperatures. Points are labelled with temperatures of extraction in degrees Celsius. (For detailed interpretation see text.)

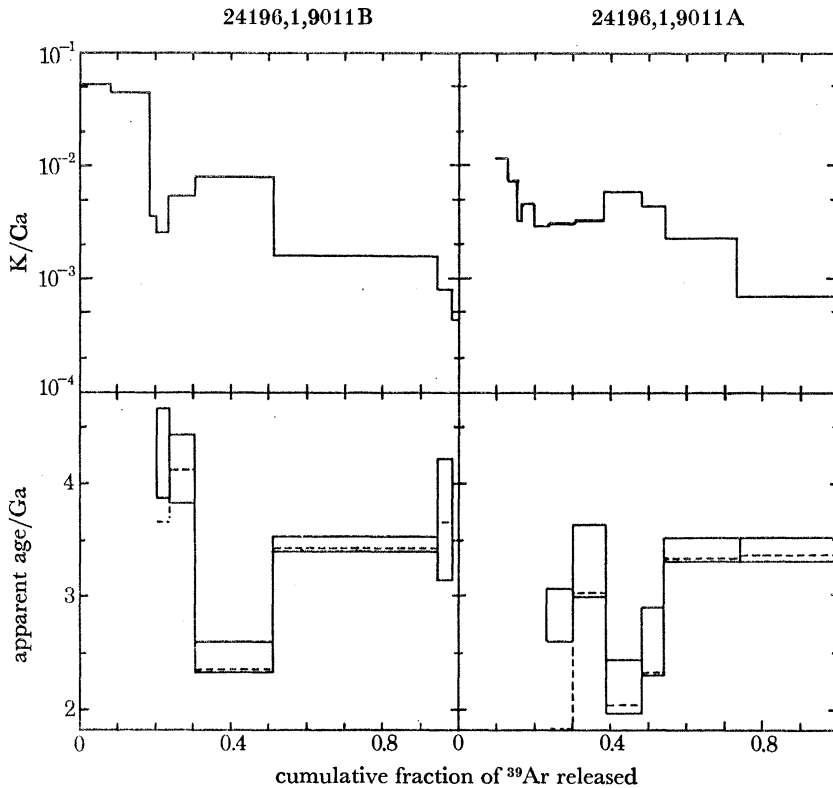


FIGURE 3. ^{40}Ar - ^{39}Ar apparent age and K/Ca release pattern for 24196A and 24196B. The mean high-temperature age is 3.36 ± 0.10 Ga. The mid-temperature decrease in apparent age may be the result of either ^{40}Ar or ^{39}Ar recoil (see text).

around 3.3 Ga, the actual value depending to some extent on assumptions about the trapped composition (see below).

The data, excluding the low-temperature solar wind dominated fractions, are displayed as an apparent age spectrum in figure 3 along with the K/Ca ratios inferred from $^{39}\text{Ar}/^{37}\text{Ar}$. The trapped ^{40}Ar correction has been made on the basis of $(^{40}\text{Ar}/^{36}\text{Ar})_t = 0.58 \pm 0.09$, inferred from the solid correlation line which passes through the high temperature points and the low temperature points with the lowest $^{40}\text{Ar}/^{36}\text{Ar}$ ratio (820 °C (A), 890 °C (A)). The effect of an alternative assumption, $(^{40}\text{Ar}/^{36}\text{Ar})_t = 0.85$ determined on the basis of the broken line in figure 2, is shown by the broken line in figure 3. Since it is likely that $(^{40}\text{Ar}/^{36}\text{Ar})_t$ decreases monotonically with increasing temperature the dashed line in figure 3 represents a realistic lower limit to the apparent age spectrum with the solid pattern being the preferred one.

The straightforward picture presented above is unfortunately compromised by the 870 °C point from 24196B. This extraction produced surprisingly little trapped argon although ^{37}Ar , cosmogenic ^{38}Ar , and ^{39}Ar were released in amount similar to the extractions before and after it. We are at a loss to understand why the trapped argon reservoir 'switched off' for just one extraction. In addition the $^{40}\text{Ar}/^{39}\text{Ar}$ ratio corresponds to an apparent age significantly higher than those of the later release fractions. Furthermore, 24196 has a very fine-grained granulitic texture (*ca.* 25 μm), which leads us to the possibility that we are observing the effects of ^{39}Ar recoil, in which case the low apparent ages for the extractions around 1000 °C may also be recoil artefacts.

This possibility, that $^{40}\text{Ar}/^{39}\text{Ar}$ has been lowered by enhanced ^{39}Ar release, gains further support from the K/Ca release pattern. $^{39}\text{Ar}/^{37}\text{Ar}$ is clearly enhanced in those fractions where $^{40}\text{Ar}/^{39}\text{Ar}$ is depressed (figure 3).

Given the complex nature of the argon release from the metabasalt, a cooling age can only be derived on the basis of unverifiable assumptions about the underlying causes of the pattern shown in figure 3. On the assumption that the low apparent ages reflect ^{40}Ar loss, cooling ages of 3.34 ± 0.11 Ga for 24196A and 3.38 ± 0.08 Ga for 24196B are calculated from the high-temperature points. On the alternative assumption that the fluctuations in apparent age are the result of ^{39}Ar recoil, cooling ages of 3.14 ± 0.16 Ga for 24196A and 3.24 ± 0.14 Ga for 24196B are calculated, based on total $^{40}\text{Ar}/^{39}\text{Ar}$ ratios obtained by summing the radiogenic ^{40}Ar and ^{39}Ar in those fractions not dominated by solar wind. Of necessity, this latter calculation must ignore the undoubted contribution of potassium derived argon (20–30 %) to the low-temperature release.

Despite the uncertainties in the above approach, the ages obtained are comparable with the precisely determined crystallization age of the layer 170 microgabbro (Lunatic Asylum 1978) and clearly suggest that the metabasalts found at the Luna 24 site were metamorphosed contemporaneously with the extrusion of the lavas in Mare Crisium. This supports the suggestion of Ryder *et al.* (1977) that they are thermally metamorphosed flow margins.

The ^{40}Ar – ^{39}Ar release patterns obtained from the separated feldspar and pyroxene from the crushed microgabbro, 24170,1–3, are displayed in figure 4 along with the variation in K/Ca ratio inferred from $^{39}\text{Ar}/^{37}\text{Ar}$. Some trapped argon was present in both samples. It represented less of a problem than for the metabasalt and the correction was made on the basis of the ratio determined for the metabasalt $(^{40}\text{Ar}/^{36}\text{Ar})_t = 0.68 \pm 0.09$.

The feldspar showed some evidence of ^{40}Ar loss in the initial extractions. The three high-temperature extractions were, within error, equal and corresponded to a crystallization age of

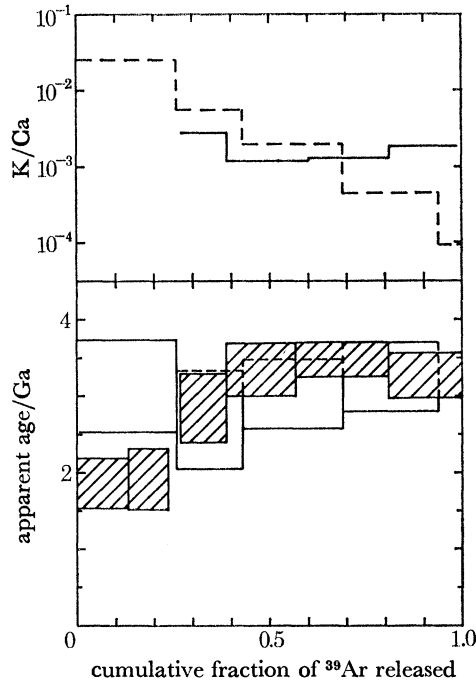


FIGURE 4. ⁴⁰Ar-³⁹Ar apparent age and K/Ca release pattern for feldspar and pyroxene separates from 24170. The mean of the three high-temperature points for the feldspar indicate an age of 3.37 ± 0.20 Ga. The mean age of all extractions for the pyroxene is 3.17 ± 0.30 Ga.

TABLE 1. K ABUNDANCES AND COSMIC RAY EXPOSURE DATA

sample	K/Ca	[Ca]† (%)	10 ⁶ [K]†	(³⁸ Ar/Ca) at s.t.p. 10 ⁻⁸ cm ³ /g	P ₃₈ (Fe)/P ₃₈ (Ca)
24196A	0.0016	≡ 8.9	140	315 ± 8	—
24196B	0.0022	≡ 8.9	195		
24170 feldspar	0.0017	≡ 13.5	230	304 ± 10	—
24170 pyroxene	0.00079	≡ 8.8	70	308 ± 10	0.006 ± 0.021
24170 whole rock‡	0.0014	8.4	120	300 ± 12	ca. 0.01
24096 fragments§	0.0021	8.3	175	914 ± 21	0.027 ± 0.011

† K abundances for the present experiment are based on K/Ca and assumed values for Ca abundance.

‡ Lunatic Asylum (1978).

§ Stettler & Albarede (1978).

|| Calculated in this paper from published data.

3.37 ± 0.20 Ga. The pyroxene extractions were also within error equal and corresponded to an age of 3.17 ± 0.30 .

The crystallization age obtained is in agreement with the more precise age of 3.30 ± 0.05 Ga reported previously (Lunatic Asylum 1978), and conveys no new information. The major features of interest in the present experiment on 24170 relate to the exposure history of the Luna 24 core, which is discussed in the next section.

Table 1 summarizes the overall K/Ca ratios and K concentrations determined for 24196 and 24170. Note that because of uncertainties in the absolute sensitivity of the spectrometer (the small sample size inhibited us from introducing large volumes of air to calibrate the spectrometer!), K concentrations are calculated on the basis of assumed values for Ca.

Cosmic ray exposure history

In addition to the solar wind component, ^{38}Ar in lunar rocks is produced by cosmic ray bombardment, the principal target elements being Ca, K, Ti and Fe. Near the surface, the galactic cosmic ray production rates per unit mass are approximately in the ratios 1 : 1 : 0.1 : 0.05. Because of its high abundance, Ca is the dominant target species, accounting usually for 85–100% of the cosmogenic ^{38}Ar production. For this reason $^{38}\text{Ar}/^{37}\text{Ar}$ ratios can be reliably used to infer cosmic ray exposure ages (Turner *et al.* 1971).

The Luna 24 VLT basalts are so low in K and Ti that production from both is negligible. The Fe/Ca ratio in VLT basalts is typically 1.8, implying that production from Fe could be 8% of the total cosmogenic ^{38}Ar . In pyroxene the proportion produced from Fe could be as much as 12% of the total. Production of ^{38}Ar from ^{56}Fe ($\Delta A = 18$) requires considerably more energetic cosmic ray protons than the production from ^{40}Ca ($\Delta A = 2$). For this reason the production rate from Fe, denoted $P_{38}(\text{Fe})$, decreases with depth in the regolith as the energetic

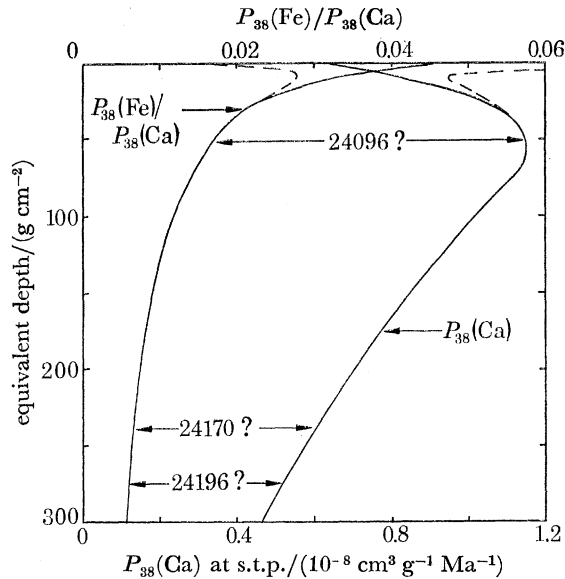


FIGURE 5. Production rate of ^{38}Ar from Ca, $P_{38}(\text{Ca})$, and relative production rates from Fe and Ca, $P_{38}(\text{Fe})/P_{38}(\text{Ca})$, plotted against equivalent depth in the lunar regolith (R. C. Reedy, personal communication). The solid curve indicates the effects due to galactic cosmic rays. The broken curve shows the effect of including solar flare protons in the calculations. Tentative assignments of Luna 24 sampling depths are also indicated.

primary cosmic ray flux is attenuated. In contrast the production rate from Ca, $P_{38}(\text{Ca})$, actually increases with depth initially, owing to the build-up of a cascade of secondary protons and neutrons. At greater depths, $P_{38}(\text{Ca})$ also decreases. Figure 5 shows the results of theoretical calculations of the variation of $P_{38}(\text{Ca})$ and $P_{38}(\text{Fe})/P_{38}(\text{Ca})$ with equivalent depth (R. C. Reedy, personal communication; Reedy & Arnold 1972). Figure 5 also shows a tentative assignment of the actual depths within the lunar regolith from which the samples analysed were derived (Bogard & Hirsch 1978). The position of the sample analysed by Stettler & Albarede (1978) (layer 24096) is also indicated. By measuring the ratio of cosmogenic ^{38}Ar to ^{37}Ar ($\equiv \text{Ca}$) in feldspar ($\text{Fe}/\text{Ca} \approx 0$) and pyroxene ($\text{Fe}/\text{Ca} \approx 2.2$) from 24170, we have attempted to estimate the value of $P_{38}(\text{Fe})/P_{38}(\text{Ca})$ appropriate to this sample. The object of

this measurement is not to determine the present position of 24170, which is of course known, but to see if there is any evidence of an earlier near-surface irradiation that could be used to constrain the deposition history of the Luna 24 regolith.

The experimental data from 24170,1–3 appropriate to the determination of $^{38}\text{Ar}_c/\text{Ca}$ is displayed in figure 6, which is a three-isotope correlation diagram of $^{38}\text{Ar}/^{36}\text{Ar}$ against $^{37}\text{Ar}/^{36}\text{Ar}$. A straight line correlation results from a simple mixture of trapped solar wind

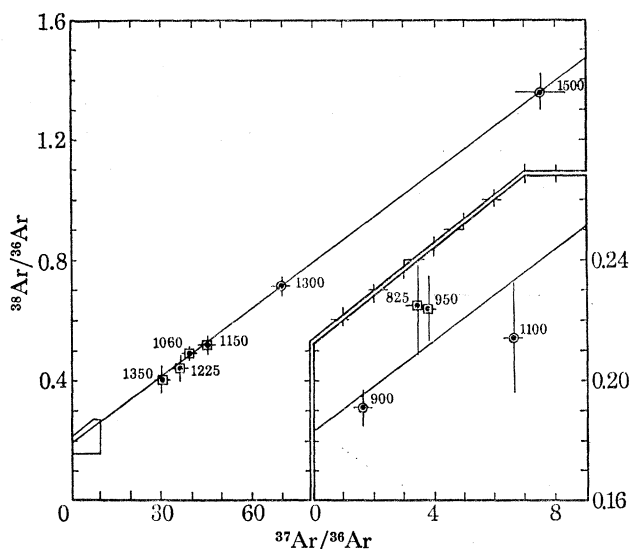


FIGURE 6. $^{38}\text{Ar}/^{36}\text{Ar}$ – $^{37}\text{Ar}/^{36}\text{Ar}$ isotope correlation for feldspar and pyroxene from 24170. The $^{38}\text{Ar}_c/^{37}\text{Ar}$ ratio is 1.132 times the slope of this graph (see text). The corresponding $^{38}\text{Ar}_c/\text{Ca}$ ratio is $(3.06 \pm 0.07) \times 10^{-6} \text{ cm}^3$ at s.t.p./g Ca. The $^{37}\text{Ar}/^{36}\text{Ar}$ ratios for the feldspar have been renormalized to the pyroxene J value before plotting. Points are labelled with temperatures of extraction ($^{\circ}\text{C}$). Circles, pyroxene; squares, feldspar.

argon ($^{38}\text{Ar}/^{36}\text{Ar} = 0.1869$; $^{37}\text{Ar}/^{36}\text{Ar} = 0$) and Ca derived argon ($^{38}\text{Ar}/^{36}\text{Ar} \approx 1.63$; $^{37}\text{Ar}/^{36}\text{Ar} \neq 0$). It is a simple matter to show that the ratio of cosmogenic ^{38}Ar to ^{37}Ar (derived from neutron activation of Ca) is obtained by multiplying the slope of figure 6 by the factor $(^{38}\text{Ar}/^{36}\text{Ar})_c / \{ (^{38}\text{Ar}/^{36}\text{Ar})_c - (^{38}\text{Ar}/^{36}\text{Ar})_t \}$, i.e. 1.132. The ratio of cosmogenic ^{38}Ar to the target Ca abundance is then obtained by using the expression

$$^{38}\text{Ar}_c/\text{Ca} = 7.012 \times 10^{-3} \alpha J (^{38}\text{Ar}_c/^{37}\text{Ar}) \text{ cm}^3 \text{ at s.t.p./g.} \quad (1)$$

This replaces the expression given in Turner (1972), following the recently recommended change in the ^{40}K decay constants (these enter the expression through the definition of J); α is the $^{37}\text{Ar}/^{39}\text{Ar}$ ratio corresponding to unit Ca/K ratio and is 0.54 for the present neutron irradiation.

The presence of Fe-derived cosmogenic ^{58}Ar would be manifested in figure 6 by some or all of the points from an iron-bearing mineral or rock lying above the line obtained from an iron-free calcium-bearing mineral from the same rock; i.e. in 24170 some or all of the pyroxene points should lie above the feldspar line. This is no evidence for such a difference between $^{38}\text{Ar}_c/^{37}\text{Ar}$ for the two minerals. Note that because of the differences in J value the $^{37}\text{Ar}/^{36}\text{Ar}$ ratios measured in the feldspar have been renormalized to the pyroxene J value before plotting.

The $^{38}\text{Ar}_c/\text{Ca}$ ratio has been calculated separately for the feldspar, $(3.04 \pm 0.10) \times 10^{-6} \text{ cm}^3$ at s.t.p./g Ca, and for the pyroxene, $(3.08 \pm 0.10) \times 10^{-6} \text{ cm}^3$ at s.t.p./g Ca, assuming

$(^{38}\text{Ar}/^{36}\text{Ar})_t = 0.1869$. These results imply that the ratio of ^{38}Ar produced from Fe in the pyroxene to that produced from Ca is (0.013 ± 0.047) . The compositions of the pyroxenes have been well documented (Lunatic Asylum 1978). They are zoned with Fe varying from 14 to 23% and Ca from 7 to 10%. Taking account of this variation we estimate a value of (2.2 ± 0.6) for Fe/Ca and obtain finally $P_{38}(\text{Fe})/P_{38}(\text{Ca}) = (0.006 \pm 0.021)$.

We have treated the published whole rock data for 24170 (Lunatic Asylum 1978) in a similar way and from a best fit to a $^{38}\text{Ar}/^{36}\text{Ar}$ - $^{37}\text{Ar}/^{36}\text{Ar}$ correlation diagram obtain $^{38}\text{Ar}_e/\text{Ca} = (3.00 \pm 0.12) \times 10^{-6} \text{ cm}^3$ at s.t.p./g Ca, which is indistinguishable from our value (the $^{38}\text{Ar}_e/\text{Ca}$ ratio implied by the Lunatic Asylum's quoted exposure age is a factor of 1.13 less than the above value for reasons which are not clear). Whole rock data for Apollo surface rocks frequently show appreciable enhancements of $^{38}\text{Ar}_e/^{37}\text{Ar}$ in the high-temperature release. Detailed examination of the Lunatic Asylum's data suggests a slight enhancement in the 1400 °C

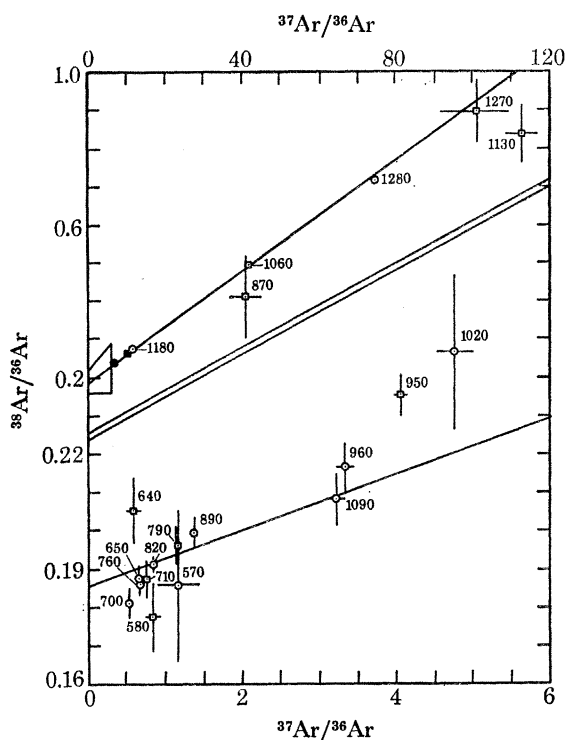


FIGURE 7. $^{38}\text{Ar}/^{36}\text{Ar}$ - $^{37}\text{Ar}/^{36}\text{Ar}$ isotope correlation for metabasalt samples 24196A (circles) and 24196B (squares). The solid symbols represent total gas compositions. The slope of the correlation line indicates a $^{38}\text{Ar}_e/\text{Ca}$ ratio of $(3.15 \pm 0.08) \times 10^{-6} \text{ cm}^3$ at s.t.p./g Ca, which is close to the value obtained for the crushed gabbro 24170. Points are labelled with temperatures of extraction in degrees Celsius. (Note: $J = 0.1010 \pm 0.0010$.)

(nominal temperature) release from both samples. The excess $^{38}\text{Ar}_e$ involved amounts to roughly 2% of the total cosmogenic ^{38}Ar and would therefore indicate $P_{38}(\text{Fe})/P_{38}(\text{Ca}) \approx 0.01$. Both experiments suggest fairly clearly that production of ^{38}Ar from Fe is significantly lower in 24170 than in surface exposed samples. Reference to figure 5 shows that this in turn implies that much of the cosmic ray exposure experience by 24170 occurred at depth.

The cosmic ray exposure data for metabasalt fragments 24196A and 24196B are displayed in figure 7. The slope of the best fit line corresponds to $^{38}\text{Ar}_e/\text{Ca} = (3.15 \pm 0.08) \times 10^{-6} \text{ cm}^3$ at s.t.p./g Ca, which is close to the value obtained for 24170. In view of the possibility that recoil

has affected the ^{39}Ar release, we have not attempted to draw any conclusions regarding Fe contributions to $^{38}\text{Ar}_c$. We note in passing that the points that depart furthest from the correlation, ($^{37}\text{Ar}/^{36}\text{Ar}$, low) are just those mid-temperature points for which $^{40}\text{Ar}/^{39}\text{Ar}$ is depressed (figure 3) and $^{39}\text{Ar}/^{37}\text{Ar}$ enhanced. Possibly recoil of ^{37}Ar is responsible.

Deposition history of the Luna 24 regolith

The numerical results of the calculations in the preceding section are summarized in Table 1. We have also re-examined the published cosmic ray exposure data of Stettler & Albarede (1978). These measurements were made on a fragment from layer 24090, which is close to the peak of the ^{38}Ar production curve (figure 4). The $^{38}\text{Ar}_c/^{37}\text{Ar}$ ratio shows a distinct increase at high temperatures, rising from $(6.48 \pm 0.15) \times 10^{-2}$ in the first 40% to $(6.98 \pm 0.16) \times 10^{-2}$ in the final 60% of ^{37}Ar release. This behaviour is typical of many surface-exposed rocks. Assuming that the high temperature increase results from Fe-derived $^{38}\text{Ar}_c$ and that $\text{Fe}/\text{Ca} = 1.8 \pm 0.2$ we infer that $P_{38}(\text{Fe})/P_{38}(\text{Ca}) = 0.027 \pm 0.011$. This is close to the value at the inferred present location of layer 24096. The low-temperature ratio, assumed to represent Ca-derived $^{38}\text{Ar}_c$ only, corresponds to $^{38}\text{Ar}_c/\text{Ca} = (0.14 \pm 0.21) \times 10^{-6} \text{ cm}^3$ at s.t.p./g Ca.

It is usual to convert $^{38}\text{Ar}_c/\text{Ca}$ ratios to cosmic ray exposure ages by using a nominal production rate of $1.4 \times 10^{-8} \text{ cm}^3$ at s.t.p. $\text{g}^{-1} \text{ Ca Ma}^{-1}$. While such a procedure may have some limited justification for surface rocks, it is clearly not appropriate to fragments from a core in which the production rate varies by a factor of 2 or more. Figure 4 shows that even for surface rocks it is a questionable procedure without some reliable 'hardness' monitor such as $P_{38}(\text{Fe})/P_{38}(\text{Ca})$.

As an alternative approach let us attempt to combine the data in table 1 with the production curve in figure 4 to place limits on the history of the Luna 24 regolith. As argued in the previous section, the low value of $P_{38}(\text{Fe})/P_{38}(\text{Ca})$ implies that 24170 received a significant proportion of its exposure at some depth below the surface. According to figure 5, the production rate at the inferred depth of 24170 is only 65% of the near surface minimum value, i.e. not more than $0.9 \times 10^{-8} \text{ cm}^3$ at s.t.p. $\text{g}^{-1} \text{ Ca Ma}^{-1}$, if the minimum is equated to the commonly used production rate of $1.4 \times 10^{-8} \text{ cm}^3$ at s.t.p. $\text{g}^{-1} \text{ Ca Ma}^{-1}$. According to Reedy's calculations, which have gained support from a recent comparison with experimental data (Hohenberg *et al.* 1978), the production rate at the depth of 24170 is actually closer to $0.6 \times 10^{-8} \text{ cm}^3$ at s.t.p. $\text{g}^{-1} \text{ Ca Ma}^{-1}$. If most of the overlying regolith were deposited at the same time as 24170, then its nominal exposure age of 500 Ma (based on Reedy's production rate) or not less than 350 Ma (based on the higher production rate) would indicate an upper limit to the time of deposition.

If the material above 24170 accumulated in several stages, this upper limit is reduced. If, as an extreme case, we assume that 24170 acquired its exposure at or just below the peak of the production curve, the upper limit is reduced to around 270 Ma (Reedy production rate) or not less than 180 Ma (based on the higher 'nominal' production rate). The only way in which 24170 can have been in its present position in the regolith for more than 500 Ma is for its depth in the regolith to have *decreased* significantly to its present value in that time.

The metabasalt has $^{38}\text{Ar}_c/\text{Ca}$ comparable with 24170, although in its location before retrieval the production rate was lower by some 20%. This suggests either that it was deposited 50–100 Ma before 24170 or it arrived at about the same time already preirradiated.

The sample from layer 24096 analysed by Stettler & Albarede (1978) has $^{38}\text{Ar}_c/\text{Ca}$ greater

by a factor of 3 than 24170. However, at its inferred location in the regolith the production rate is close to its maximum value. This implies that the 24096 layer cannot have existed in its present location for longer than 790 Ma (or not less than 514 Ma). This is older than the limit already imposed by 24170 and suggests that the fragment arrived in the 24096 layer with a pre-exposure of at least 30 %.

One should not attempt to read too much into the measurements of only three fragments. Clearly individual fragments with the lowest exposure in any regolith layer give the most useful information about the deposition history of that layer. Therefore the picture inferred will always face the possibility of change should a younger fragment be found in a particular layer. Nevertheless it is tempting to speculate, from the way in which $^{38}\text{Ar}_c/\text{Ca}$ and $P_{38}(\text{Fe})/P_{38}(\text{Ca})$ follow the broad trend of the instantaneous production profiles, despite pre-irradiation effects, that the regolith at Luna 24 has existed in more or less its present form for the last 350–500 Ma. Bogard & Hirsch (1978) concluded, from a detailed study of grain size separates, that the Luna 24 regolith had accumulated in complex way from material with a preirradiation history over a period of the order of 300 Ma. This time scale is broadly consistent with our findings.

SUMMARY AND CONCLUSIONS

The experiments described above on small lithic fragments from the Luna 24 core have provided useful information about several aspects of the basalts in Mare Crisium and the regolith layer at the landing site. The major conclusions that can be drawn are as follows.

1. ^{40}Ar – ^{39}Ar analysis of a metabasalt fragment with a fine-grained granulitic texture showed the effects of implanted solar wind argon and disturbances in the $^{40}\text{Ar}/^{39}\text{Ar}$ ratio resulting either from ^{40}Ar loss or ^{39}Ar recoil. Based on extreme assumptions, the cooling age was inferred to be between 3.36 ± 0.11 Ga (high-temperature release) and 3.14 ± 0.16 Ga (cumulative $^{40}\text{Ar}/^{39}\text{Ar}$ ratio). This is comparable with the age of a crystalline microgabbro in the Luna 24 core and supports the suggestion that the metabasalts represent thermally metamorphosed flow margins rather than the product of later impact events.

2. Separated minerals from the layer 170 microgabbro gave ages of 3.37 ± 0.20 Ga (feldspar) and 3.17 ± 0.30 Ga (pyroxene). These are in agreement with a more precise 'whole rock' age of 3.30 ± 0.05 Ga for the microgabbro (Lunatic Asylum 1978), but do not permit any new conclusions to be drawn.

3. We have demonstrated how a comparison of the ratio of cosmogenic ^{38}Ar to the major target element Ca, in separated minerals from the core, can be used to determine relative production rates from Fe and Ca, and have shown for the first time that, by comparing these with theoretical production profiles, one can obtain information about the depth–time history of the sample. The relative production ratio, $P_{38}(\text{Fe})/P_{38}(\text{Ca})$, for the layer 170 microgabbro is very low, 0.006 ± 0.021 , indicating a 'soft' irradiation spectrum and implying that the gabbro received most of its cosmic ray exposure at depth in the core. Application of the same reasoning to published data on a basalt from layer 096 indicates a 'harder' irradiation spectrum. $P_{38}(\text{Fe})/P_{38}(\text{Ca})$ calculated for that sample, 0.027 ± 0.011 , is slightly higher but comparable with the present-day production ratio at the depth of layer 096. This implies that the fragment in question obtained most of its cosmic ray exposure close to the surface.

4. Taking account of the variation of production rate with depth, the measured ratio, $^{38}\text{Ar}_c/\text{Ca} = (3.06 \pm 0.10) \times 10^{-6}$ cm³ at s.t.p./g Ca, for the microgabbro indicates that it has

spent no more than 500 Ma in its present location. This in turn implies that the overlying regolith was deposited more recently. The metabasalt gave a similar value for ³⁸Ar_c/Ca, $(3.15 \pm 0.08) \times 10^{-6}$ cm³ at s.t.p./g Ca. The *present-day* production rate of ³⁸Ar_c in layer 196, from which the metabasalt came, is 20% lower than in layer 170 and the measured ³⁸Ar_c/Ca could therefore imply that it was deposited 50–100 Ma before the metabasalt or that it was deposited at the same time with a previous history of cosmic ray exposure.

The exposure ages, taken in conjunction with the approximate agreement between measured production *ratios* and present-day production ratios, tentatively suggest that much of the Luna 24 core has remained undisturbed for the last 350–500 Ma.

We wish to thank the Academy of Sciences of the U.S.S.R. for generously providing the Luna 24 samples. We wish also to thank David Blagburn for his help with the mass spectrometry and Mrs Elaine Lycett for typing the manuscript. We also acknowledge support from the Natural Environment Research Council through a research grant (GR3/1715).

REFERENCES

- Blanchard, D. P., Haskin, L. A., Brannon, J. C. & Aaboe, E. 1977 Chemistry of soils and particles from Luna 24 (abstract). In *Papers Presented to the Conference on Luna 24*, pp. 18–21. Houston: Lunar Science Institute.
- Bogard, D. D. & Hirsch, W. C. 1978 Noble gases in Luna 24 core soils. In *Mare Crisium: the view from Luna 24* (ed. R. B. Merrill & J. J. Papike), pp. 105–116. New York: Pergamon.
- Cadogan, P. H. & Turner, G. 1977 ⁴⁰Ar–³⁹Ar dating of Luna 16 and Luna 20 samples. *Phil. Trans. R. Soc. Lond. A* **284**, 167–177.
- Graham, A. L. & Hutchison, R. 1980 Mineralogy and petrology of fragments from the Luna 24 core. *Phil. Trans. R. Soc. Lond. A* **297**, 15–22 (this volume).
- Head, J. W., Adams, J. B., McCord, T. B., Pieters, C. & Zisk, S. 1978 Regional stratigraphy and geologic history of Mare Crisium. In *Mare Crisium: the view from Luna 24* (ed. R. B. Merrill & J. J. Papike), pp. 43–74. New York: Pergamon.
- Hohenberg, C. M., Marti, K., Podosek, F. A., Reedy, R. C. & Shirck, J. R. 1978 Comparisons between observed and predicted cosmogenic noble gases in lunar samples. In *Proc. Lunar planet. Sci. Conf. 9th*. New York: Pergamon. (In the press.)
- Lunatic Asylum 1978 Petrology, chemistry, age and irradiation history of Luna 24 samples. In *Mare Crisium: the view from Luna 24* (ed. R. B. Merrill & J. J. Papike), pp. 657–678. New York: Pergamon.
- Ma, M.-S. & Schmitt, R. A. 1977 Luna 24 soils: a chemical study (abstract). In *Papers Presented to the Conference on Luna 24*, pp. 102–105. Houston: The Lunar Science Institute.
- Reedy, R. C. & Arnold, J. R. 1972 Interaction of solar and galactic cosmic ray particles with the moon. *J. geophys. Res.* **77**, 537–555.
- Ryder, G., McSween Jr, H. Y. & Marvin, U. B. 1977 Basalts from Mare Crisium. *Moon* **17**, 263–287.
- Schaeffer, O. A., Bence, A. E., Eichhorn, G., Papike, J. J. & Variman, D. T. 1978 ³⁹Ar–⁴⁰Ar and petrologic study of Mare Crisium: age and petrology of Luna 24 samples 24077,13 and 24077,63 (abstract). *Lunar Sci.* **9**, 1007–1009. Houston: Lunar Science Institute.
- Staudacher, T., Jessberger, E. K., Dörflinger, D. & Kiko, J. 1978 A refined ultrahigh-vacuum furnace for rare gas analysis. *J. Phys. E* **11**, 781–784.
- Steiger, R. H. & Jäger, E. 1977 Subcommittee on Geochronology: convention on the use of decay constants in geo- and cosmochronology. *Earth planet. Sci. Lett.* **36**, 359–362.
- Stettler, A. & Albarede, F. 1978 Ar³⁹–Ar⁴⁰ systematics of two mm-sized rock fragments from Mare Crisium. *Earth planet. Sci. Lett.* **38**, 401–406.
- Taylor, G. J., Warner, R. D., Wentworth, S., Keil, K. & Sayeed, U. 1978 Luna 24 lithologies: Petrochemical relationships among lithic fragments, mineral fragments, and glass. In *Mare Crisium: the view from Luna 24* (ed. R. B. Merrill & J. J. Papike), pp. 303–320. New York: Pergamon.
- Turner, G. 1972 ⁴⁰Ar–³⁹Ar age and cosmic ray irradiation history of the Apollo 15 Anorthosite 15415. *Earth planet. Sci. Lett.* **14**, 169–175.
- Turner, G., Huneke, J. C., Podosek, F. A. & Wasserburg, G. J. 1971 ⁴⁰Ar–³⁹Ar ages and cosmic ray exposure ages of Apollo 14 samples. *Earth planet. Sci. Lett.* **12**, 19–35.
- Turner, G., Enright, M. C. & Cadogan, P. H. 1978 The early history of chondrite parent bodies inferred from ⁴⁰Ar–³⁹Ar ages. In *Proc. Lunar planet. Sci. Conf. 9th*. New York: Pergamon. (In the press.)